

Collision-Induced Spectra of the Helium Isotopes

Michael H. Proffitt, J. W. Keto, and Lothar Frommhold

Physics Department and Electronics Research Center, University of Texas at Austin, Austin, Texas 78712

(Received 25 July 1980)

Gas-phase Raman spectra of the diatoms $^3\text{He}_2$ and $^4\text{He}_2$ are measured, the former for the first time. The *depolarized* spectra of the collisional pairs are in near agreement with computations based on a recent configuration-interaction calculation of the helium-diatom polarizability (anisotropic part). The *polarized* spectra, however, require a somewhat more substantial trace than the configuration-interaction prediction. Measurements of the second virial dielectric coefficient support this conclusion.

PACS numbers: 33.70.-w, 34.10.+x, 35.20.My

The Raman process of diatomic molecules is well understood.¹ Its generalization to free atoms in a collisional encounter, which undergo transitions between translational states when interacting with photons, is called "collision-induced scattering of light." It was first demonstrated by McTague and Birnbaum² using conventional Raman apparatus and rare-gas targets. At not too high densities observed intensities vary as the *square* of the gas density, because of the diatomic origin. The spectra, which are of a roughly exponential shape, can be computed from wave-mechanical theory if "models" of the diatom polarizability invariants are known.³

Diatom polarizability is that portion of the pair polarizability which arises from the interaction. It is given by the polarizability of two interacting atoms, minus the polarizabilities of the separated pair. The tensor components are functions of the separation R of the atoms. The invariants, trace and anisotropy, determine the shapes and intensities of polarized and depolarized Raman spectra, respectively. The diatom polarizability is also related to the second virial coefficients of (a) the dielectric Clausius-Mosotti function, (b) the refractive Lorenz-Lorentz relation, and (c) the Kerr effect.³

Existing self-consistent-field (SCF) and configuration-interaction (CI) type calculations of the helium-diatom polarizability are reviewed elsewhere.³ Measurements are sparse and quite difficult because of the smallness of the quantity. We report here the first measurement using the rare isotope ^3He . Improved diatom spectra of ordinary ^4He are also given. For direct comparison with these new measurements we compute line shapes using the CI data as input. The only other measurements related to the helium diatom polarizability are those of the dielectric second virial coefficient,^{4,5} and earlier ^4He Raman spectra.⁶⁻⁸ Two of these were recorded at high den-

sities^{7,8} and are now known to suffer from three-body interference.⁹ The attempt to extract the depolarized *diatom* spectrum from the high-pressure data by means of a virial analysis resulted, however, in a spectrum which is roughly 40% more intense than our measurement.⁹ (The other high-pressure data⁸ are consistent with our calibration, except for small deviations due to three-body effects at low frequencies.) We can not explain the nature of this inconsistency, but point out that the isotope spectra of $^3\text{He}_2$ provide an independent test of the ^4He spectra.

We note the diatom polarizabilities of ^3He and ^4He are very nearly identical. On the other hand, the isotope spectra differ, because of two facts. The *mass difference* leads to more broad-banded spectra for the lighter isotope. Because of *nuclear spin*, different symmetries of the pair wave functions result. For the boson, ^4He , only even angular momentum quantum numbers are allowed. Interacting fermions like ^3He , on the other hand, are three times more likely found with odd angular momentum (just like orthohydrogen is three times more abundant than parahydrogen). Even though the differences due to symmetry disappear at high temperatures, at room temperature a small effect is observable. The question we address is whether the different spectra can be fitted with the *same* model of the polarizability.

A conventional 90° -scattering Raman apparatus⁶ is used, with a laser beam of about 2 W at 5145 Å wavelength parallel to the x axis of a Cartesian frame. The direction of observation is that of the y axis. The beam polarization is normally vertical, parallel to the z axis, but can be rotated with a half-wave plate when desired. Gas densities of about 30 amagats are used. Signals vary as the square of the density, with no three-body contributions detected. Ratios of anti-Stokes and Stokes intensities are consistent with the Boltzmann factor. The common isotope ^4He was obtained with

total impurities amounting to less than 1 ppm, with nitrogen as the major contaminant. The rare isotope ^3He was cleaned by flowing first over titanium at 900°C , followed by oxygen-free copper at 4.2 K. The apparatus used ultra-high vacuum techniques and was tested by cleaning a sample of ^4He to which we purposely added N_2 impurities. A 1 m double monochromator with holographic gratings was used, with slits set to 4 cm^{-1} . A polarization scrambler (quartz wedge) was attached to the first slit.

For each isotope two spectra, S_{\parallel} and S_{\perp} , were recorded, one with the beam polarization parallel and the other perpendicular to the direction of observation, as shown in Fig. 1. (To offset the spectra in the figure, ^3He intensities are multiplied by a factor of 10.) Absolute intensity scales are obtained relative to the accurately known spectrum of the argon diatom. We note that the ^4He intensities are 16% lower than previously reported,⁶ because of a monochromator leadscrew error that was recently discovered. [For comparison with the present spectra, our previous data⁶ must be scaled by an additional factor $(4880/5145)^4 = 0.81$ to account for the different excitation wavelengths, 4880 instead of 5145 \AA .]

The isotope spectra look similar but differ significantly. For example, the inverse logarithmic slopes of S_{\parallel} at low frequencies are 59 and 52 cm^{-1} for ^3He and ^4He , respectively. Even greater differences are observed for the slopes of S_{\perp}

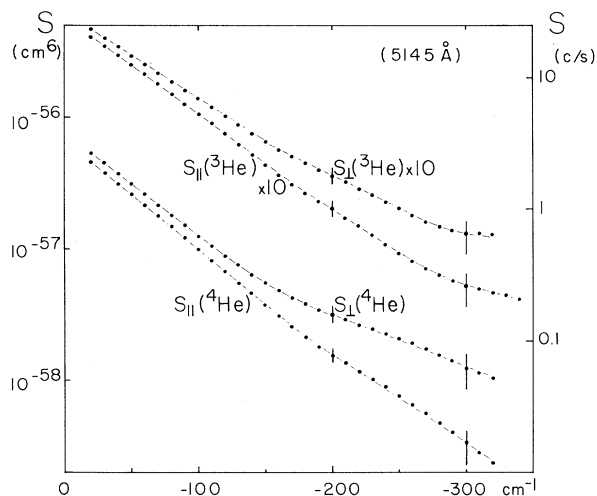


FIG. 1. Collision-induced diatom Raman spectra (Stokes side) of the helium isotopes. Excitation wavelength is 5145 \AA ; polarization of the incident beam is parallel (S_{\parallel}) and perpendicular (S_{\perp}). ^3He intensities are multiplied by 10.

(66 and 56 cm^{-1}). At low frequencies, the ^3He intensities are up to 12% smaller than the ^4He spectra, much more than the experimental uncertainty of $<2\%$. At the high frequencies, the ^4He intensities are up to 30% smaller than comparable ^3He signals. Considering next the differences between S_{\parallel} and S_{\perp} for each isotope separately, we note that particularly at the high frequencies, totally different logarithmic slopes are observed. This indicates the presence of a polarized spectrum. The signals are the superposition of a polarized (P) and a depolarized (D) component, as in

$$S_{\parallel} = aP + D \quad \text{and} \quad S_{\perp} = P + bD,$$

with known coefficients a and b .³ That system of equations can be solved for P and D , see Figs. 2 and 3 (dots). At low frequencies, the depolarized spectrum has small statistical uncertainties of 2%. On an absolute scale, the error is believed to be less than 6%. The weak polarized spectrum, as a difference of two nearly identical numbers, is necessarily more uncertain.

We proceed to compare our experimental results with the fundamental theory. The only CI

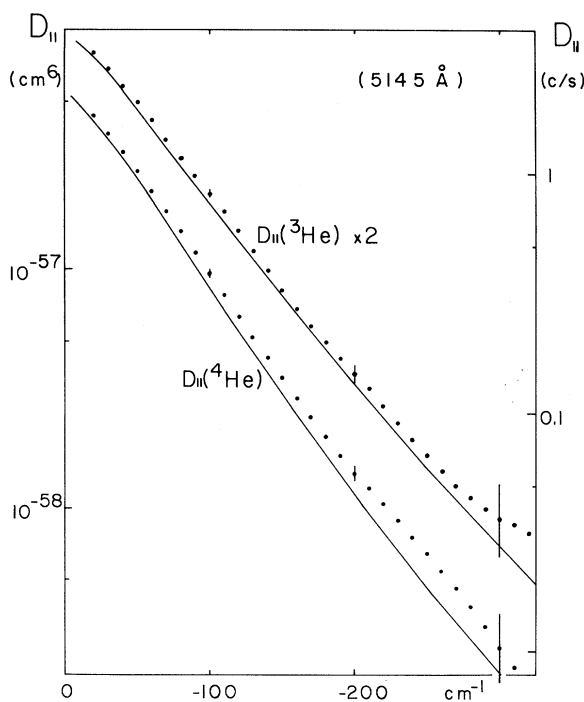


FIG. 2. Measurement (dots) of the *depolarized* Raman spectra of the helium diatoms, $^3\text{He}_2$ and $^4\text{He}_2$. Also shown (curve) is the wave-mechanical computation based on a CI calculation of the diatom polarizability (Ref. 10).

helium-diatom polarizability data¹⁰ known to date are used for that purpose. The traditional theory of the Raman process of diatomic molecules was extended to include the free state of two atoms.³ Relevant matrix elements of trace and anisotropy are computed by numerical integration of Schrödinger's equation of relative atomic motion, with use of an established semiempirical interaction potential.¹¹ (Other refined potentials give virtually identical results.³) The resulting profiles are also shown in Figs. 2 and 3. We note that the theoretical polarizabilities are static, but the experiment measures dynamic (i.e., frequency dependent) values. However, the expected differences amount to only 1%–3%, that is less than the experimental error, and will be ignored here.

Theory and depolarized spectra are in near agreement. They differ by 10% or even less at the lower frequencies, but most of the observed difference is significant. The measurement will be used elsewhere to obtain an improved, empirical anisotropy.

For the weak polarized spectra, we find a near-consistency within the much bigger errors, although the experiment indicates higher intensities than the CI theory suggests. It is interesting to mention, therefore, that measurements of the second dielectric coefficient B_ϵ of ⁴He likewise

indicate that the CI trace is too small. The overlap of the two measurements^{4,5} is $B_\epsilon = -0.095 \pm 0.005 \text{ cm}^6 \text{ mol}^{-2}$, which we compare with the number obtained for the CI trace: $-0.058 \text{ cm}^6 \text{ mol}^{-2}$. The experimental facts call for a trace model, which is roughly 1.5 times the CI trace. The experiments are thus in better agreement with the SCF calculations than with CI.³ Dacre¹⁰ pointed out that the effect of including electron correlation is to make the trace less negative, which changes the virial coefficient from -0.09 to $-0.06 \text{ cm}^6 \text{ mol}^{-2}$, which, however, is seen to be inconsistent with the measurements.

In summarizing, we see that the measurements of the helium-isotope-diatom polarizability are mutually consistent. The spectra are also consistent with the measurements of the virial dielectric coefficient. Furthermore, line-shape computations based on the CI anisotropy agree very nearly with the depolarized spectra. The weak trace spectra are, however, at best marginally consistent with the CI theory. All measurements considered, it appears that the (dynamic) trace is about 1.5 times the CI data. It is thus more nearly in agreement with the SCF trace data. This surprising result can, maybe, be understood in this way: The trace is known to depend to a much higher degree on the exact electronic overlap. An accurate calculation is, therefore, more difficult than that of the anisotropy, for which these contributions largely cancel.^{3,10} Furthermore, the trace amounts to only 1% or so of the anisotropy. Since both invariants are computed with the same numerical precision, the relative uncertainty of the trace is much larger. The inclusion of electron correlation is known¹⁰ to increase the anisotropy by about 10%, which does clearly improve the SCF values to near perfection.

The support of the Joint Services, Electronics Program, and of the Robert A. Welch Foundation, is gratefully acknowledged.

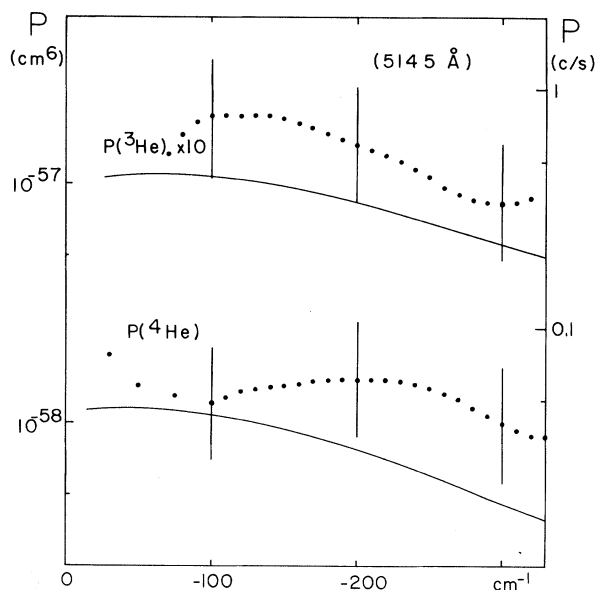


FIG. 3. Measurements (dots) of the polarized Raman spectra of the helium diatoms, ³He₂ and ⁴He₂. Also shown (curve) is the wave-mechanical computation based on a CI calculation of the diatom polarizability (Ref. 10).

¹A. Weber, in *The Raman Effect*, edited by A. Anderson (Marcel Dekker, New York, 1973), Chap. 9.

²J. P. C. McTague and G. Birnbaum, *Phys. Rev. A* **3**, 1376 (1971).

³L. Frommhold, *Adv. Chem. Phys.* **46**, 1 (1980).

⁴R. H. Orcutt and R. H. Cole, *J. Chem. Phys.* **46**, 697 (1967).

⁵D. Vidal and P. M. Lallemand, *J. Chem. Phys.* **64**, 4293 (1976).

⁶M. H. Proffitt and L. Frommhold, *J. Chem. Phys.* **72**, 1377 (1980).

⁷F. Barocchi, P. Mazzinghi, and M. Zoppi, *Phys. Rev. Lett.* **41**, 1785 (1978).

⁸Y. LeDuff, *Phys. Rev. A* **20**, 48 (1979).

⁹F. Barocchi and M. Zoppi, talk given at the Interna-

tional Conference on Collision-Induced Phenomena, Florence, Italy, 2-5 September, 1980 (to be published).

¹⁰P. D. Dacre, *Mol. Phys.* **36**, 541 (1978).

¹¹R. A. Aziz, V. P. S. Nain, J. S. Carley, W. L. Taylor, and G. T. McConville, *J. Chem. Phys.* **70**, 4330 (1979).

Observation of the Transition from Uncollapsed to Collapsed Excited f -Wave Functions in I^- , Xe, and Cs^+ via the Giant Post-Collision-Interaction Auger Effect

T. -C. Chiang,^(a) D. E. Eastman, F. J. Himpsel, G. Kaindl,^(b) and M. Aono^(c)
IBM Thomas J. Watson Research Center, Yorktown Heights, New York 10598

(Received 30 May 1980)

The nature of the final f -wave functions, i.e., spatially collapsed versus uncollapsed, involved in $4d \rightarrow 4f$, ϵf giant absorption resonances in I^- , Xe, and Cs^+ is revealed by studying the post-collision interaction (PCI) in the $N_{4,5}O_{2,3}O_{2,3}$ Auger decay of the $4d$ hole. While small PCI Auger shifts ≈ 0.2 eV are observed for I^- and Xe with uncollapsed f -wave functions, a giant PCI Auger shift of ~ 1 eV is observed for Cs^+ with collapsed f -wave functions.

PACS numbers: 32.80.Hd, 79.60.Eq

Giant absorption resonances associated with $4d \rightarrow 4f$, ϵf optical transitions in Xe and Xe-like ions have been of continuing theoretical and experimental interest for the past decade.¹⁻⁵ The resonances for atomic numbers $Z \leq 54$ (I^- , Xe, etc.) are mainly described as due to the delayed onset of $4d \rightarrow \epsilon f$ continuum transitions, while the resonances for $Z > 55$ (Ba^{++} , La^{+++} , etc.) are generally described as mainly due to a $4d \rightarrow 4f$ (1P_1 channel) discrete transition which is raised into the f continuum by the exchange interaction.² The essential physical difference between these two cases is the spatial extent of the major contributing final wave functions, i.e., uncollapsed f -wave functions for $Z \leq 54$ versus collapsed f -wave functions for $Z > 55$.⁵ The delineation of these two cases, especially for $Z = 55$ (Cs^+), is a challenging problem, and has attracted much theoretical attention.¹⁻⁵ Previous studies have concentrated on the absorption profiles which are, however, not very sensitive to these differences. In this Letter, we report a new measure of these $4f$, ϵf -wave functions via studies of the $h\nu$ -dependent post-collision interaction (PCI)⁶ associated with the Auger decay of the $4d$ hole. Small "ordinary" PCI interactions are observed for uncollapsed final f -wave functions while giant PCI interactions are observed for collapsed final f -wave functions. The changeover is abrupt, and provides a direct proof that f -wave-function collapse has occurred

for Cs^+ .

Figure 1(a) shows the giant absorption resonances associated with $4d \rightarrow 4f$, ϵf transitions for I^- , Xe, and Cs^+ in solid KI, Xe, and $CsCl$, respectively.^{1,7} The $N_{4,5}$ thresholds for excitation of $4d_{3/2,5/2}$ core levels to the vacuum level are indicated, and are obtained from the photoemission measurements to be discussed below. Except for small overlapping fine structures due to excitonic transitions and solid-state effects,^{1,7} the absorption profiles vary smoothly with Z as far as the widths and heights are concerned. Thus, a qualitative inspection of the profiles does not reveal the nature of the final f -wave functions involved. From atomic calculations in the independent particle model, the final f -radial-wave function sees a two-well potential due to the combination of Coulomb and centrifugal terms.^{1,3,4} For $Z \leq 54$, the potential barrier between the two wells generally acts to repel the f electron from the core region. Thus, continuum ϵf -wave functions just above threshold have little amplitude in the core region, as shown schematically in Fig. 2. The giant absorption comes about when the energy of the ϵf electron is high enough to penetrate the barrier and overlap appreciably with the $4d$ -core wave function (Fig. 2); at still higher energies, the rapid oscillation of the ϵf -wave function in the core region quenches the transition. For $Z > 55$, the inner potential well becomes deep and